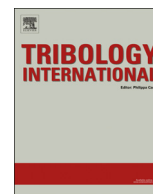




ELSEVIER

Contents lists available at ScienceDirect

Tribology International

journal homepage: [www.elsevier.com/locate/triboint](http://www.elsevier.com/locate/triboint)

# Improving the tribological characteristics of piston ring assembly in automotive engines using Al<sub>2</sub>O<sub>3</sub> and TiO<sub>2</sub> nanomaterials as nano-lubricant additives

Mohamed Kamal Ahmed Ali<sup>a,c,\*</sup>, Hou Xianjun<sup>a,\*\*</sup>, Liqiang Mai<sup>b</sup>, Cai Qingping<sup>a</sup>, Richard Fiifi Turkson<sup>a,d</sup>, Chen Bicheng<sup>a</sup>

<sup>a</sup> Hubei Key Laboratory of Advanced Technology for Automotive Components, Wuhan University of Technology, Wuhan, 430070 China

<sup>b</sup> State Key Laboratory of Advanced Technology for Materials Synthesis and Processing, Wuhan University of Technology, Wuhan, 430070 China

<sup>c</sup> Automotive and Tractors Engineering Department, Faculty of Engineering, Minia University, El-Minia, 61111 Egypt

<sup>d</sup> Mechanical Engineering Department, Ho Polytechnic, P.O. Box HP 217, Ho, Ghana

## ARTICLE INFO

### Article history:

Received 28 June 2016

Received in revised form

27 July 2016

Accepted 5 August 2016

Available online 9 August 2016

### Keywords:

Nano-lubricant additives

Nano-tribology

Piston ring assembly

Friction

Wear

## ABSTRACT

To minimize the frictional power losses in automotive engines, it is imperative to improve the tribological characteristics of the piston ring assembly. This study examined the tribological behavior of the piston ring assembly using nanoparticles as nano-lubricant additives. The average size of Al<sub>2</sub>O<sub>3</sub> and TiO<sub>2</sub> nanoparticles were 8–12 nm and 10 nm, respectively. The nanoparticles were suspended using oleic acid in four different concentrations in the engine oil (0.05, 0.1, 0.25 and 0.5 wt%). The tribological behavior of nano-lubricants was evaluated using a tribometer under different operating conditions to mimic the ring/liner interface. The results showed a decrease in the friction coefficient, power losses and wear. The study provides insights into how nano-lubricant additives could contribute towards energy saving and improved fuel economy in automotive engines.

© 2016 Elsevier Ltd. All rights reserved.

## 1. Introduction

Existing and future automotive engines would require more efficient engine oils, a situation that presents a new challenge for researchers and designers with regard to finding ways of enhancing the tribological characteristics of internal combustion engines while achieving a reduction in fuel and lube oil consumption. Most designers and researchers have focused on Nano tribology in internal combustion engines as the key strategy for minimizing frictional power losses, excessive heat generation and the wear of contact surfaces, in a manner that will ultimately lead to an improved performance of automotive engines. The piston ring assembly makes a significant contribution towards the total frictional power losses. The power losses in automotive engines vary between 17% and 19% of the total energy generated [1]. An improvement in the tribological performance of the lubricating oils and the piston ring assembly leads to an improved efficiency and fuel economy of engines because the friction between the piston

ring and the liner accounts for almost 40–50% of the power losses [2,3]. Furthermore, controlling friction via the use of nano-lubricants leads to a decline in the level of wear and an increase in the service intervals for which an oil change is required. This ultimately translates into minimized maintenance costs.

The lubrication is classified into three general regimes: boundary, mixed, and elastohydro-dynamic/ hydrodynamic [4]. During one stroke, the different lubrication regimes can occur over the stroke depending on running conditions. Boundary or mixed lubrication regimes occur near the top and bottom dead center of stroke (TDC and BDC), with the hydrodynamic lubrication regime occurring at mid-stroke [2]. Nevertheless, hydrodynamic friction increases under the conditions of high speeds and low loading [5]. The total friction of the piston ring assembly comprises boundary friction at asperity contact locations (TDC and BDC) and viscous friction due to shearing of lubricant. The boundary lubrication can occur if the oil film becomes thin enough. The load is carried on the surface peaks and not by the lubricant film. For this reason, nano-lubricant additives are most effective under boundary lubrication conditions as it forms a tribofilm at the asperity contact locations to separate the sliding surfaces [6].

Recently, nanoparticles have attracted increasing interest and have been used in a lot of energy related fields owing to their unusual electrical, mechanical and piezoelectric properties [7]. The

\* Corresponding author at: Hubei Key Laboratory of Advanced Technology for Automotive Components, Wuhan University of Technology, Wuhan 430070, China.

\*\* Corresponding author.

E-mail addresses: [eng.m.kamal@mu.edu.eg](mailto:eng.m.kamal@mu.edu.eg) (M.K.A. Ali), [houxj@whut.edu.cn](mailto:houxj@whut.edu.cn) (H. Xianjun).

nanoparticles could be used as nano-lubricant additives in automotive engines to improve the tribological performance, oil properties, exhaust emission, combustion, saving fuel and enhance heat transfer rate. The addition of nanomaterials to lubricating oils can effectively improve the tribological properties through the formation of a protective film on surfaces and creating a rolling effect between friction surfaces [8,9]. Nanomaterials are different from traditional bulk materials because they possess high specific surface areas and extremely small sizes. The selection of nanomaterials is a very important step towards the improvement of the tribological performance and enhancing the properties of engine oils [10]. Re-formation of solid-like tribo-films by the nanoparticles on the friction surfaces is not possible at high speeds when the lubricant film thickness is larger than the nanoparticles diameter [11]. The bearing and sliding between the nanoparticles play the main role in lowering the friction and wear between worn surfaces [12]. Furthermore, the lower elastic modulus and the comparatively higher magnitude of hardness possessed by nanomaterials can be considered as the main reasons for the excellent lubricating properties [13].

Aluminum and titanium oxides ( $\text{Al}_2\text{O}_3$  and  $\text{TiO}_2$ ) nanoparticles are the most appropriate for many environmental applications due to their excellent tribological, chemical and thermal properties [14]. The addition of  $\text{TiO}_2$  nanoparticles with lubricant oil showed stable friction due to the formation of protective films on worn surfaces [15]. Shenoy et al. [16] investigated the influence of  $\text{TiO}_2$  nanoparticles additives in lube oil. The results exhibited a higher load bearing capacity by a margin of 35% compared to the use the lube oil without nanoparticle addition. Friction and wear experiments were conducted by Kao and Lin [17] using a reciprocating sliding tester. The average diameter of  $\text{TiO}_2$  was 50 nm and 5 wt% particle concentration in the rapeseed oil. The results revealed that there was an 80.84% reduction in mean surface roughness. The coefficient of friction and the wear scars decreased approximately by 15.2% and 11%, respectively [18]. Mohan et al. [19] studied the influence of the addition of  $\text{Al}_2\text{O}_3$  nanoparticles to lubricating oil (SAE 20W40). The results illustrated that using 20 nm of grain size for a 0.5% wt% could reduce the friction by 49.1% and 21.6% under flooded and starved conditions, as compared to the lubricant without nanoparticles. Another study also demonstrated that using 40–80 nm of grain size  $\text{Al}_2\text{O}_3$  nanoparticles at 5 wt% concentration reduced of the wear rate [20].

The agglomeration of the nanoparticles in engine oil inhibits their free motion and eliminates the mechanism of nanoparticles (the transfer nanoparticles from engine oil to rubbing surfaces to form tribofilm and produce a rolling effect). Therefore, the nanoparticles were added to the engine oil with different solvents to disperse the particles to form stable suspensions for a more effective operation [21,22]. Gulzar et al. [23] added 1 wt% of oleic acid to nanoparticles for the purpose of suspension and the reduction of agglomerates. The results suggested that adding oleic acid reduced of the wear. The results from the experimental work carried out by Luo et al. [24] exhibited that the average reduction of the friction coefficient was 17.61% for the four-ball test and 23.92% for the thrust-ring test, for a 0.1 wt% concentration and 78 nm grain size of  $\text{Al}_2\text{O}_3$  nanoparticle addition to the oil. Using a low concentration of  $\text{TiO}_2$  nanoparticles is enough for improving the tribological characteristics [25]. Vashghani et al. [26] investigated the effect of tiny  $\text{Al}_2\text{O}_3$  nanoparticles on engine oil properties. The results presented that the thermal conductivity improved by 37.49% using 3 wt% concentrations. Nanoparticles can easily enter into small gaps between sliding surfaces because of their ultrafine sizes, whereas the micron-scale traditional additives cannot [27].

The objectives of the current study include the formulation of  $\text{Al}_2\text{O}_3$  and  $\text{TiO}_2$  nano-lubricants and the investigation of the

tribological characteristics of a piston ring assembly under different running conditions such as contact loads, reciprocating sliding speeds, sliding distance and concentration of nanoparticles. In addition, more investigations were performed using field emission scanning electron microscopy (FE-SEM), energy dispersive spectroscopy (EDS), X-ray photoelectron spectroscopy (XPS) and non-contact 3D surface profiler for analyzing the worn surfaces to understand the major mechanisms leading to improve the tribological behavior of piston ring assembly in automotive engines using  $\text{Al}_2\text{O}_3$  and  $\text{TiO}_2$  nano-lubricant additives.

## 2. Experimental section

### 2.1. Materials

Against the background that  $\text{Al}_2\text{O}_3$  and  $\text{TiO}_2$  are the most appropriate for many tribological applications (including solid lubricants) because of their excellent tribological behavior, these nanoparticles were chosen for the current investigation.  $\text{Al}_2\text{O}_3$  and  $\text{TiO}_2$  powders were purchased from Nanjing XFNANO Materials Tech Co., Ltd. The average sizes of the  $\text{Al}_2\text{O}_3$  and  $\text{TiO}_2$  nanoparticles were 8–12 nm and 10 nm, respectively. The varying concentrations of  $\text{Al}_2\text{O}_3$  and  $\text{TiO}_2$  used were 0.05, 0.1, 0.25 and 0.5 wt% in the engine oil for each nanoparticle type. The tribological tests were conducted using of engine oil (Castrol EDGE professional A5 5W-30, a commercial lubricant) to demonstrate the effect of using nanoparticles as engine oil additives. Table 1 shows the compositions of the tested samples of  $\text{Al}_2\text{O}_3$  and  $\text{TiO}_2$  nano-lubricants.

### 2.2. Dispersibility of $\text{Al}_2\text{O}_3$ and $\text{TiO}_2$ nanoparticles in engine oil

The mixing of nanoparticles with the engine oil is an important step towards the improvement in the engine oil quality. Oleic acid was used as a surface modifier and to ensure proper dispersion of  $\text{Al}_2\text{O}_3$  and  $\text{TiO}_2$  nanoparticles within the engine oil, a magnetic stirrer was used for blending the nanoparticles and the engine oil for 4 h with the aim of obtaining a homogeneous and stable suspension. Oleic acid plays the important role of blending the nanoparticles in a manner that makes them soluble in the engine oil. The oleic acid provides stability for the nanoparticles, preventing the agglomeration of the nanoparticles within engine oils [28]. In the current study, the UV–visible spectroscopy and dynamic light scattering (DLS, Zetasizer Nano ZS system) method were used to elucidate the colloidal stability of  $\text{Al}_2\text{O}_3$  and  $\text{TiO}_2$  nano-lubricant samples.

The absorption spectra of the nano-lubricants were measured directly after preparation (at time=0). As shown in Fig. 1(a), the  $\text{Al}_2\text{O}_3$  and  $\text{TiO}_2$  nano-lubricant sample colors appeared uniform in color. It was obvious that the engine oil containing oleic acid was brighter and had a clear yellow color. The comparison between the UV absorbance peaks was conducted to monitor the stability of the

**Table 1**  
The compositions of nano-lubricants.

Concentration (wt%)	Standard oil (5W-30)	Additive solution
<b>0.05</b>	98% Oil	2% $\text{TiO}_2$ or $\text{Al}_2\text{O}_3$ Solution (0.05% nanoparticles + 1.95% oleic acid)
<b>0.1</b>	98% Oil	2% $\text{TiO}_2$ or $\text{Al}_2\text{O}_3$ Solution (0.1% nanoparticles + 1.9% oleic acid)
<b>0.25</b>	98% Oil	2% $\text{TiO}_2$ or $\text{Al}_2\text{O}_3$ Solution (0.25% nanoparticles + 1.75% oleic acid)
<b>0.5</b>	98% Oil	2% $\text{TiO}_2$ or $\text{Al}_2\text{O}_3$ Solution (0.5% nanoparticles + 1.5% oleic acid)

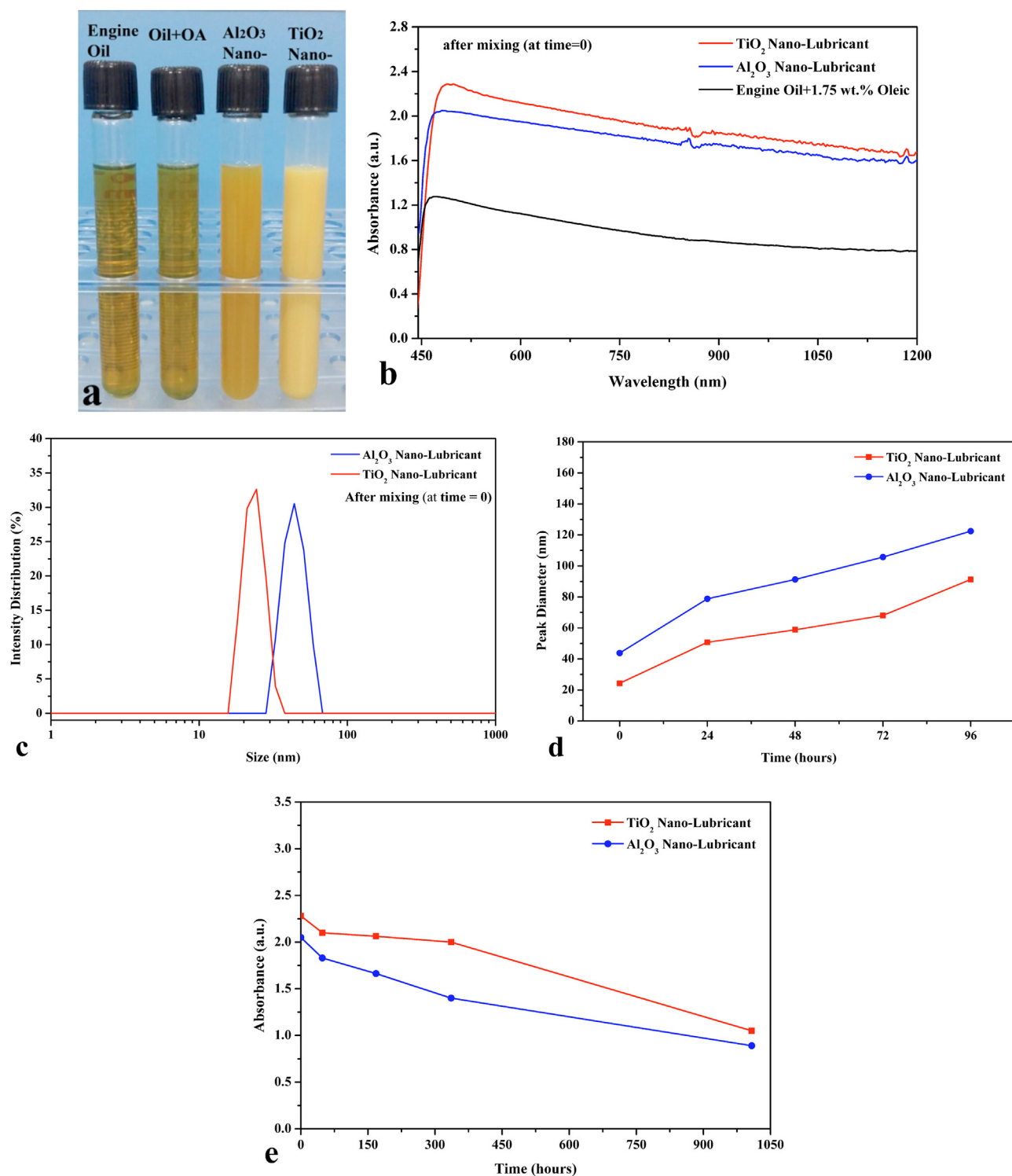


**Fig. 1.** (a) Photograph of nano-lubricant samples, (b) UV for nano-lubricants (0.25 wt% nanoparticles) and engine oil with oleic acid after preparation (at time=0), (c) Peak size distribution for Al<sub>2</sub>O<sub>3</sub> and TiO<sub>2</sub> nanoparticles in nano-lubricants measured by DLS after preparation (t=0), (d) Peak diameter of the Al<sub>2</sub>O<sub>3</sub> and TiO<sub>2</sub> nanoparticles in nano-lubricants as a function of time, (e) UV for Al<sub>2</sub>O<sub>3</sub> and TiO<sub>2</sub> nano-lubricants as a function of time.

Al<sub>2</sub>O<sub>3</sub> and TiO<sub>2</sub> nano-lubricants. Fig. 1(b) shows the effect of adsorbent content on the colorant behavior of nano-lubricants. A peak at wavelength of ( $\lambda_{max}$ ) of 490 and 482 nm were observed in the spectrum of TiO<sub>2</sub> and Al<sub>2</sub>O<sub>3</sub> nano-lubricants, respectively. However, the peak of the engine oil containing oleic acid without nanoparticles (470 nm) was lower than the others. The higher peak of absorbance level suggests a better distribution of the nanoparticles within the engine oil. Therefore, TiO<sub>2</sub> nano-lubricant

showed a better dispersion with time than that of Al<sub>2</sub>O<sub>3</sub> nano-lubricants.

Besides, the size of Al<sub>2</sub>O<sub>3</sub> and TiO<sub>2</sub> nanoparticles in suspensions (nano-lubricants) was measured by using a DLS method to elucidate the colloidal stability of the Al<sub>2</sub>O<sub>3</sub> and TiO<sub>2</sub> nano lubricants. The particles size distribution curves of Al<sub>2</sub>O<sub>3</sub> and TiO<sub>2</sub> nanoparticles in engine oil after immediate preparation is shown in Fig. 1(c). The initial measurement (time=0) shows the peak

diameters for  $\text{Al}_2\text{O}_3$  and  $\text{TiO}_2$  nanoparticles were 43.82 nm and 24.36 nm respectively, which were larger than the primary sizes of each particle mentioned earlier ( $\text{Al}_2\text{O}_3=8\text{--}12$  nm and  $\text{TiO}_2=10$  nm). This can translate into slight agglomeration of the nanoparticles in the engine oil due to strong Van der Waals interactions (intermolecular forces). The nanoparticle sizes of  $\text{Al}_2\text{O}_3$  and  $\text{TiO}_2$  in the engine oil also increased with time because of the sedimentation as shown in Fig. 1(d), but did not form large clusters in engine oil.

As can be seen from Fig. 1(e), the nano-lubricants were somewhat stable over a time period of 336 h (14 days) at room temperature. However, the stability was not good with the increase of the storage time because of aggregation of the nanoparticles. As evidenced by a decrease in optical absorbance and an increase in DLS peak diameter (Fig. 1(d and e)). The aggregation occurred whenever the Brownian motion and the attractive forces (Van der Waals) of the nanoparticles were greater than the repulsive forces. In the present investigation, the agglomeration of nanoparticles was reduced via the use of a magnetic stirrer for 30 min again just before the start of the tribological experiments to limit aggregation and sedimentation of the nanoparticles in engine oil. Further investigation will be required to address the sedimentation problem of the nano-lubricants to analyze influencing factors affecting the dispersion stability for longer periods.

### 2.3. Tribotest rig description

Bench tribometer test are designed to mimic the sliding reciprocating motion of the piston ring/cylinder liner interface in an engine according to ASTM G181 [29]. Fig. 2 illustrates the designed piston ring/cylinder liner bench tribometer. A 1.5 kW variable speed AC motor was used to turn the crankshaft, the speed of which was measured by a digital tachometer (HT-4200). The piston ring was placed under the pivot arm above a reciprocating cylinder liner segment in a specially designed piston ring holder. The application of the normal load to the piston ring and cylinder was via the use of dead weights at the end of an arm. A two-axes piezoelectric force transducer and charge amplifier were used to measure the normal contact and friction force generated on the piston ring during sliding. During the friction test, the signals generated were received and processed using the DEWEsoft 6.6.7 program for data acquisition connected to a PC for displaying real time variables of the experiment. The friction coefficient was automatically recorded for many cycles of crankshaft rotation. For the test rig, the inertia forces due to mass reciprocating motion were balanced via counterweights in the crankshaft webs. A large

crankshaft pulley acted as an inertia disk to minimize the angular speed variations. Furthermore, the test rig was mounted on a special table in order to ensure the damping of the vibration in a manner that resulted in stability during operation.

The test specimens of the ring and liner were fragments from actually fired engine components, to ensure that the materials used for the tests are the same as those found in an engine. The piston ring pack consists of the compression rings and oil control rings. In this set-up, the compression ring was used in the tribological tests. The test specimens and profile of the running face for the piston ring is shown in Fig. 3. The surface hardness of the ring and the liner samples was measured according to stipulated standards [30]. The average hardness of the ring surface was 320 VH (Vickers hardness), whilst the hardness for liner was 413 VH.

### 2.4. Tribological testing

The important parameters which were measured and calculated to assess the tribological performance of nano-lubricants during experiments included the friction coefficient, power losses and the wear rate of the ring. To study the effects of load and speed on the tribological parameters between the piston ring/liner interface, the load was varied from 30 to 250 N, which corresponds to contact pressures ranging from 0.65 to 5.43 MPa, respectively, to clarify the lubrication regimes. However, this does not represent typically maximum pressures under normal running conditions for the engine [31]. However, a range of contact pressures (0.65–5.43 MPa) is represented the nominal radial pressure applied after combustion at 50% of maximum engine load [32]. This is due to the combustion pressure in engine acting primarily on the piston crown and the backside and top surface of the first ring in the ring pack. To estimate the resulting contact force between the ring to the liner is the difference between these pressures. The speed was varied from 50 to 800 r.p.m, corresponding to maximum mid-stroke velocities from  $0.212\text{ m s}^{-1}$  to  $3.48\text{ m s}^{-1}$ , respectively. The stroke length was fixed at 65 mm. The average reciprocating sliding velocity of the ring can be calculated with the known running speed, connecting rod length, and crank radius [33]. The tribological experiments were conducted at an oil temperature of  $100\text{ }^\circ\text{C}$ , to simulate top dead center (TDC) position near the surface of the cylinder liner temperature [34].

In this study, the compression ring was used for the tribological tests. The compression rings in the ring pack operate under oil starvation in most of the strokes because of the action of the oil scraper ring. This presents a prolonged mixed lubrication regime during the reciprocating stroke [35,36]. In lubricant starvation, the

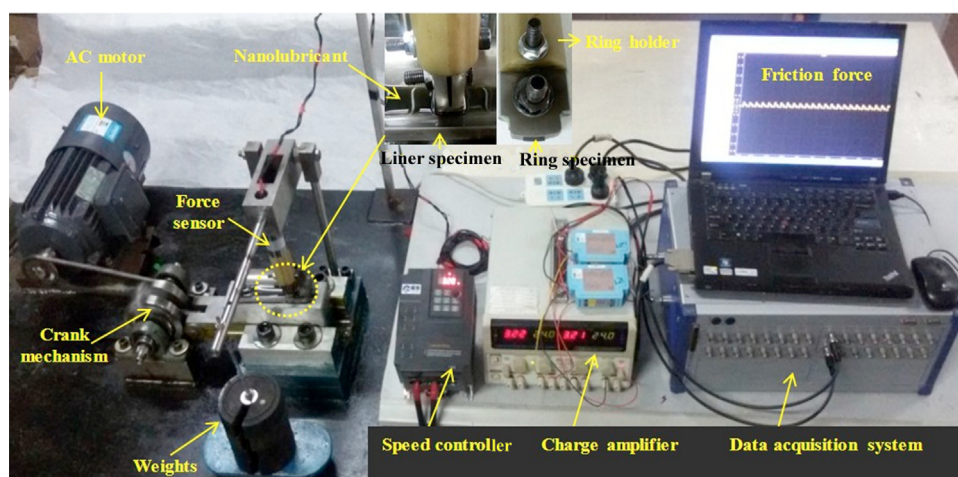


Fig. 2. The designed bench tribometer of the piston ring/cylinder liner interface.

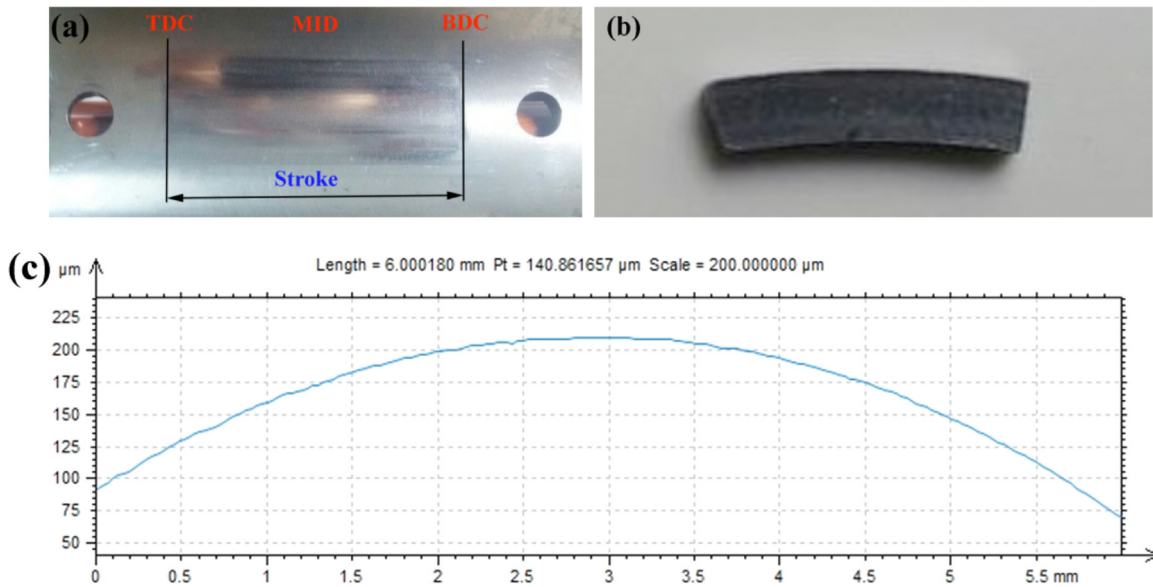


Fig. 3. The test specimens (a, b) and profile of running face for piston ring (c).

pressure of the lubricant in the outlet region does go down drastically [37]. Consequently, to simulate the characteristics of the compression ring lubrication under oil starvation, the amount of lubricant supplied to the interface between the ring and the liner should be limited to a small amount (4 ml). Moreover, the effect of lubricant starvation greatly reduces the film thickness, and is likely that this starvation condition could help in confirming the effect nano-lubricants.

Before testing for wear, piston ring specimens were ultrasonically cleaned in acetone for 15 min and dried to remove any contamination on surfaces. The wear results during this investigation have been presented in terms of specific wear rate which were calculated using the following formula:

$$\text{Specific wear rate} = \frac{V}{F_n S} \quad (1)$$

where,  $V$  is worn volume ( $\text{mm}^3$ ),  $F_n$  is the applied load on ring (N) and  $S$  is the sliding distance (m).

The extent of wear for the ring was determined via the profiles of the worn scar cross-section measured using a surface profilometer. A details description of this measurement was published in [34]. Each friction test was carried for duration of 20 min. The friction and wear tests were carried out at least three times under the same conditions in an attempt to replicate experimental results, after which the average results were taken to minimize measurement error.

### 2.5. Worn surface analysis

The wear mode and tribo-film formation on the piston ring and cylinder liner surfaces for the use of nano-lubricants and lubricating oil without nanoparticle additives were investigated. Morphologies of the worn surfaces of the ring and the liner samples were examined using field-emission scanning electron microscopy (FE-SEM, ZEISS ULTRA PLUS). The deposition of the nanoparticles on worn surfaces (tribo-film) was examined via energy dispersive spectroscopy (EDS, Inca X-Act). The chemical characterization of the boundary tribo-film on worn surface of the piston ring was analyzed by X-Ray Photoelectron Spectrometry (XPS, Thermo model ESCALAB250). The Crystalline structures and phases of the  $\text{Al}_2\text{O}_3$  and  $\text{TiO}_2$  nanoparticles were determined by X-ray diffraction (XRD) test using  $\text{CuK}\alpha$  radiation at 30 kV and 40 mA

at a scanning speed of  $0.01^\circ\text{s}^{-1}$ . The XRD data was analyzed with the assistance of MDI Jade 6 program. In addition, the surface roughness of the frictional specimens (piston ring and liner) was measured using a Nanovea ST400 3D Profilometer (non-contact profilometer). The morphological evolution of worn surfaces was conducted after a sliding distance of 15 km under a 120 N contact load and  $0.5 \text{ m s}^{-1}$  average sliding speed.

## 3. Results and discussion

### 3.1. Characterization of $\text{Al}_2\text{O}_3$ and $\text{TiO}_2$ nanoparticles

The FE-SEM images in Fig. 4 illustrate the morphology of the nanostructures for the  $\text{Al}_2\text{O}_3$  and  $\text{TiO}_2$  nanoparticles. The morphology of the  $\text{Al}_2\text{O}_3$  and  $\text{TiO}_2$  nanoparticles was fairly spherical, which provided a very good rolling medium within the engine oil. The XRD pattern of  $\text{TiO}_2$  nanoparticles in the current investigation is shown in Fig. 5. It can be observed that the peak details are  $2\theta = 25.2^\circ, 36.9^\circ, 48^\circ, 53^\circ, 55^\circ$  and  $62^\circ$  with strong diffraction peaks at  $25^\circ$  and  $48^\circ$ . The most pronounced peaks are indexed according to the JCPDS card No. 21-1272 which corresponds to the pure anatase phase, confirming that the  $\text{TiO}_2$  was in the anatase structure phase. Additionally,  $\text{Al}_2\text{O}_3$  nanoparticles also showed typical diffraction peaks (311), (400) and (441) at  $2\theta = 37^\circ, 45^\circ$  and  $67^\circ$ , respectively. From the spectra, the intensity of XRD peaks for  $\text{TiO}_2$  and  $\text{Al}_2\text{O}_3$  were such that the  $\text{Al}_2\text{O}_3$  nanoparticles had broader diffraction peaks (suggesting poor crystallization), indicating the presence of ultra-fine size crystallites [38]. It can therefore be said that the high degree of broadness of the diffraction peaks for the  $\text{Al}_2\text{O}_3$  additive was due to a less degeneracy in the crystallites ( $\text{Al}_2\text{O}_3$  being smaller than  $\text{TiO}_2$ ).

### 3.2. Effect of $\text{Al}_2\text{O}_3$ and $\text{TiO}_2$ nanoparticles concentration on friction

The nanoparticle concentration is an essential matter because they can act negatively if there is a surplus of nanoparticles. The tribological tests were conducted to assess the nano-lubricants using  $\text{Al}_2\text{O}_3$  and  $\text{TiO}_2$  nanoparticle additives in different concentrations (0.05, 0.1, 0.25 and 0.5 wt%). Fig. 6 displays the effect of nanoparticles concentration on friction coefficient for an average sliding speed of  $0.5 \text{ m s}^{-1}$  and a contact load of 120 N over a

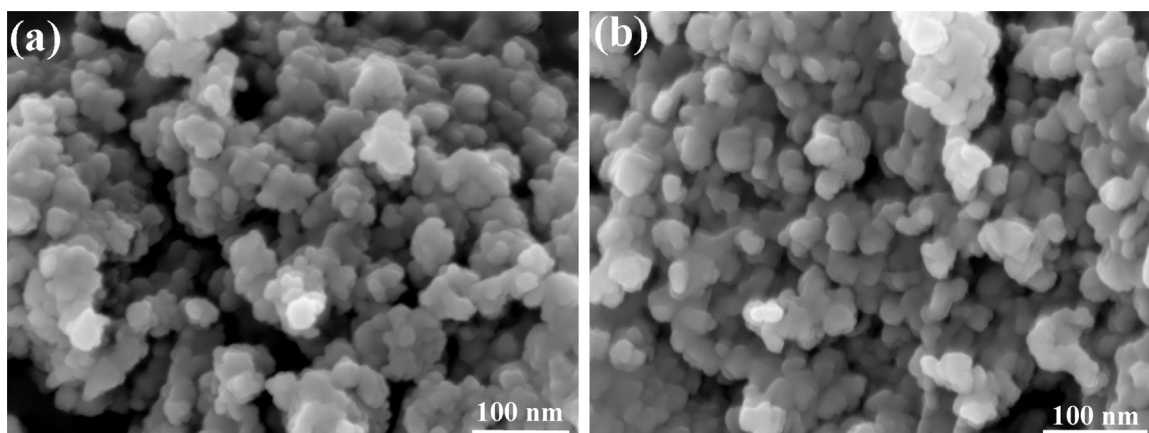


Fig. 4. FE-SEM micrographs for (a) Al<sub>2</sub>O<sub>3</sub> nanoparticles and (b) TiO<sub>2</sub> nanoparticles.

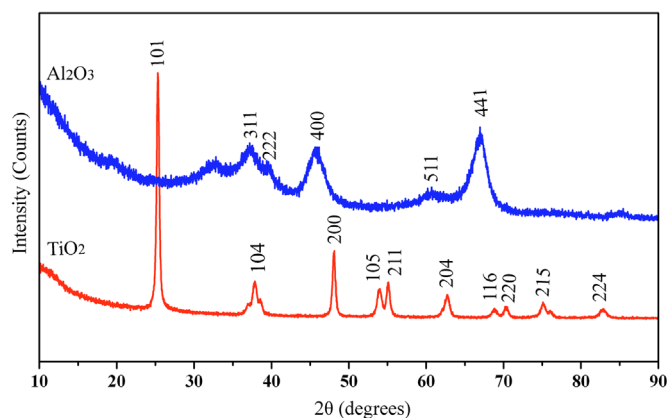


Fig. 5. XRD patterns of Al<sub>2</sub>O<sub>3</sub> and TiO<sub>2</sub> nanoparticles.

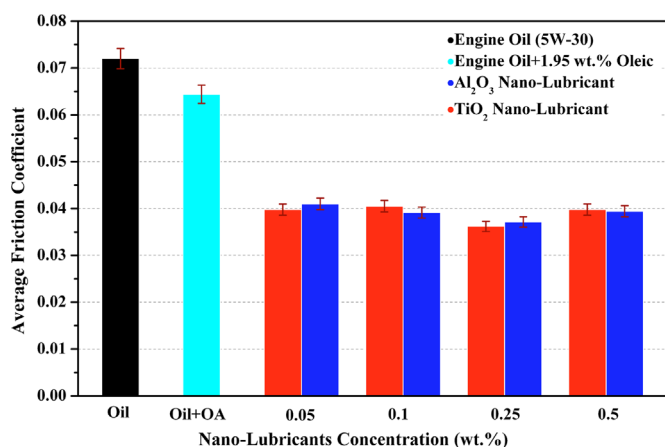


Fig. 6. Effect of Al<sub>2</sub>O<sub>3</sub> and TiO<sub>2</sub> nanoparticle concentrations on friction coefficient of the piston ring assembly.

20 min period. All concentrations of Al<sub>2</sub>O<sub>3</sub> and TiO<sub>2</sub> nano-lubricants showed a decrease in the friction coefficient. Al<sub>2</sub>O<sub>3</sub> and TiO<sub>2</sub> nano-lubricants had a reduced friction coefficient by approximately 48–50% with 0.25 wt% concentration of nanoparticles. Based on the obtained results, it was evident that the nano-lubricant with 0.25 wt% concentration of nanoparticles was the best sample of the nano-lubricants considered, as this sample minimized the friction coefficient by half, as compared with engine oil (5W-30) without nanoparticles. So, the optimum concentration (0.25 wt%) of Al<sub>2</sub>O<sub>3</sub> and TiO<sub>2</sub> nanoparticles, for the current study, was consistent with literature reports [14]. Against this

background, the optimum concentration was used for the investigation of the tribological performance in the current study. Moreover, the addition of oleic acid alone without nanoparticles reduced the friction by 11% at a concentration of 1.95 wt% in the engine oil; friction reduction was not due to physical adsorption of oleic acid on worn surfaces, but to its chemical reaction as shown by other authors [39].

### 3.3. Effect of Al<sub>2</sub>O<sub>3</sub> and TiO<sub>2</sub> nano-lubricants on viscosity and viscosity index

The kinematic viscosity and viscosity index for the engine oil with oleic acid and Al<sub>2</sub>O<sub>3</sub> and TiO<sub>2</sub> nano-lubricants was presented in the current investigation in comparison with the engine oil (5W-30) under 40 °C and 100 °C temperatures using an optimum concentration (0.25 wt%) of nanoparticles. The kinematic viscosity and viscosity index of nano-lubricants measured was based on the GB/T265-1988 and GB/T1995-1998 lubricant testing standards. Generally, the kinematic viscosity of engine oil decreased with increasing temperature. The kinematic viscosity of TiO<sub>2</sub> and Al<sub>2</sub>O<sub>3</sub> nano-lubricants recorded at the temperatures of 40 °C and 100 °C slightly decreased as shown in Fig. 7. The reason for this viscosity reduction is due to the nanoparticles coming between the lube oil layers leading to the ease of the relative movement between nano-lubricant layers and the nanoparticles acting as a catalyst [40]. Moreover, the spherical nature of the nanoparticles plays an important role in rheological behavior (viscosity). The mechanism for the reduction of the viscosity using spherical nanoparticles in the fluid can be found in the work conducted by Elena et al. [41]. On the other hand, the viscosity of an engine oil containing oleic acid was decreased by only by a small amount.

Low viscosity helps to minimize the viscous friction. Also, the viscosity reduction of the nano-lubricants confirms the Al<sub>2</sub>O<sub>3</sub> and TiO<sub>2</sub> nanoparticles effect alone for minimizing asperity friction, which is important for reducing the frictional power losses. Moreover, the results showed that the viscosity index of the nano-lubricants was increased by 1.84% as compared with that of the engine oil without nano-lubricant additives. The increase in the viscosity index indicates a more stable kinematic viscosity with temperature change, which provides better resistance to thinning of the lubricant film and fuel economy in an automotive engine.

### 3.4. Tribological performance of Al<sub>2</sub>O<sub>3</sub> and TiO<sub>2</sub> nano-lubricants

Fig. 8 presents the friction coefficient and frictional power loss characteristics during one cycle of the crankshaft for an average sliding speed of 0.65 m s<sup>-1</sup> and 120 N contact load using the best concentration of nanoparticles (0.25 wt%). The variation in the

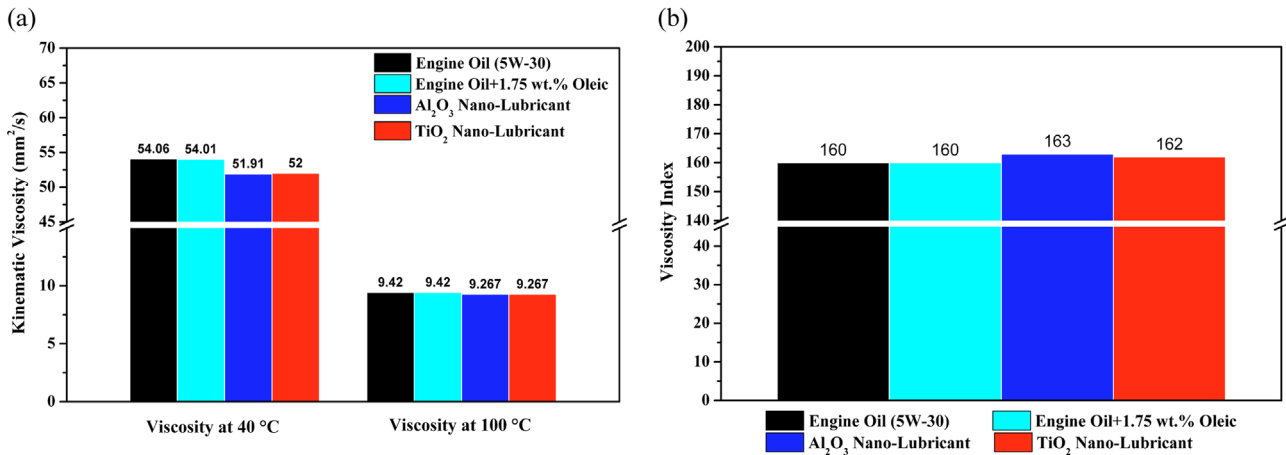


Fig. 7. Effect of Al<sub>2</sub>O<sub>3</sub> and TiO<sub>2</sub> nano-lubricants on kinematic viscosity (a) and viscosity index (b).

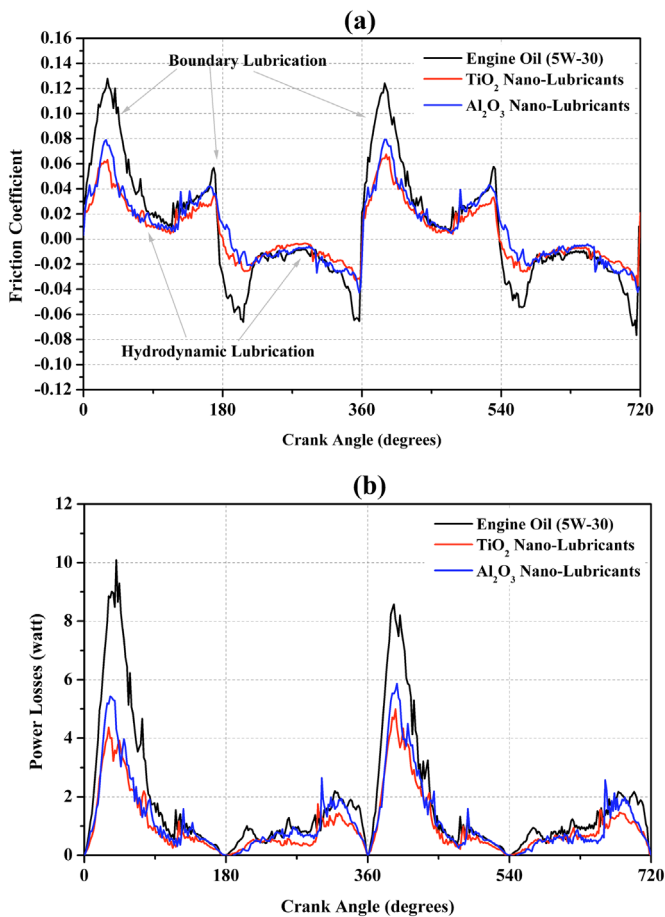


Fig. 8. Tribological behavior of piston ring assembly versus crank angle with and without the use of nanoparticles as engine oil additives under the boundary lubrication regime: (a) Friction coefficient and (b) Frictional power losses.

friction coefficient with crank angle, represented by the negative part of the curve is due to the change in sliding speed direction during the reciprocating sliding motion (Fig. 8(a)). The mechanism of the friction different during one stroke owing to different lubrication regimes can occur in the stroke depending on running conditions. The boundary or mixed lubrication regimes occur near TDC and BDC, with hydrodynamic lubrication occurring at mid-stroke.

The results showed that the maximum friction coefficient value was reached at TDC and BDC locations. The reason is related to the

critically low sliding speed attained at dead centers, which prevents adequate access of the lube oil to these locations (boundary or mixed lubrication) and the increase in the metal contact between worn surfaces (boundary lubrication). However, at the middle of the stroke minimum values of the friction coefficient were recorded because of the adequate access of the lube oil (hydrodynamic lubrication) as a result of the maximum sliding speed. In contrast, the maximum power losses were observed at mid-stroke location as shown in Fig. 8(b). This might be due to the sliding speed reaching its maximum at mid-stroke causing an increase in the shear stress in the lubricant film, leading to an increase in the frictional power losses. This behavior reveals an interesting aspect of the action of nano-lubricants.

Nano-lubricants are more effective at TDC and BDC positions during boundary and mixed lubrication regimes (Fig. 8(a)). It can be observed that the friction coefficient was reduced for Al<sub>2</sub>O<sub>3</sub> and TiO<sub>2</sub> nano-lubricants. Furthermore, the frictional power losses were reduced by 45% and 50% for the Al<sub>2</sub>O<sub>3</sub> and TiO<sub>2</sub> nano-lubricants respectively, as compared to the commercial lubricant (5W-30). The friction coefficient and power losses were reduced because of the mechanism of the nanoparticles (converting sliding into rolling friction) and the formation of tribo-films on the sliding surfaces. This reduction in frictional power losses could further enhance the automotive engine efficiency.

From the experimental results, it was observed that the friction coefficient and frictional power losses do not remain constant as explained in the modeling results obtained the work done by Ali and Zhao [2,42], but rather oscillates significantly with crank angle or time because of the stick-slip phenomenon during the sliding motion. During the stick phase, the friction force reaches a maximum value, but when slip occurs there is a decrease in the friction force owing to the energy released between the worn surfaces. The stick-slip phenomenon may result from friction surface inhomogeneity and from nonlinear properties of the equations of motion for sliding [43].

The Stribeck curve obtained from the friction experiments is shown in Fig. 9. This test allowed the evaluation of the tribological performance of nano-lubricants under different lubricating conditions. In these tests, the average reciprocating sliding speed was constant and the viscosity values as shown in Fig. 7, the Stribeck curve presented here only involved the effect of the load. This approach allowed the determination of a particular lubrication mode as well as the range of friction coefficients. In order to maintain the boundary lubrication regime, the load was kept high. The Stribeck parameter [44,45] is defined here as:

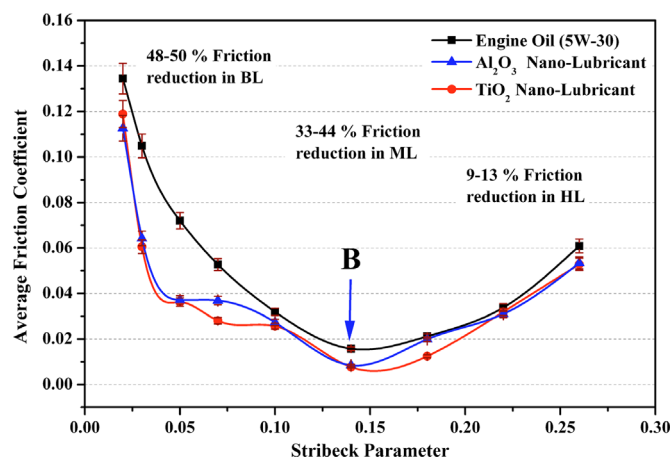


Fig. 9. Experimental Stribeck curve for piston ring assembly, with and without the use of nanoparticle engine oil additives.

$$\text{Stribeck parameter} = \frac{\text{dynamic viscosity} \times \text{sliding velocity}}{\text{load unit}} \quad (2)$$

The results showed that the use of nano-lubricants reduced the friction coefficient by 48–50%, 33–44% and 9–13% under boundary, mixed and hydrodynamic lubrication, respectively. The transition for point (B) implies that there is a shift of friction coefficient from mixed to approximately hydrodynamic (Fig. 9) as a result of the micro-polishing effect of nanoparticles as is evident in Fig. 15. A positive effect of the transition (B) will occur at a lower Stribeck parameter and leads to a reduction in wear during the boundary and mixed lubrication regimes.

Fig. 10 shows the influence of  $\text{Al}_2\text{O}_3$  and  $\text{TiO}_2$  nano-lubricants on the wear rate of the ring as compared with engine oil without nanoparticle additives. The comparison was made for different sliding distances and for a fixed contact load of 232 N. The results revealed a decrease in the wear rate for the use of  $\text{Al}_2\text{O}_3$  and  $\text{TiO}_2$  nano-lubricants by 21% and 29%, respectively, as compared with the use of engine oil without nanoparticle additives over a sliding distance of 50 km. In addition, the investigation was performed using engine oil with oleic acid to evaluate the real influence of the nanoparticles on the wear rate of the ring. The wear rate of the ring was slightly reduced by 2.6% after 50 km sliding via the addition of oleic acid to engine oil, which demonstrates the effective role of nano-lubricants on the wear rate of the ring.

To illustrate the effect of sliding speed on friction coefficient and wear rate of the piston ring when using the lubricant without nanoparticles (5W-30) and that with nanoparticles under different

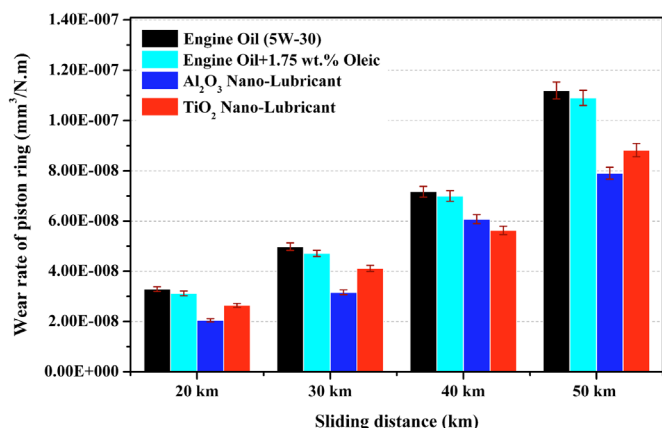


Fig. 10. Comparison of wear rate for  $\text{Al}_2\text{O}_3$  and  $\text{TiO}_2$  nano-lubricants with engine oil (5W-30) under a contact load of 232 N.

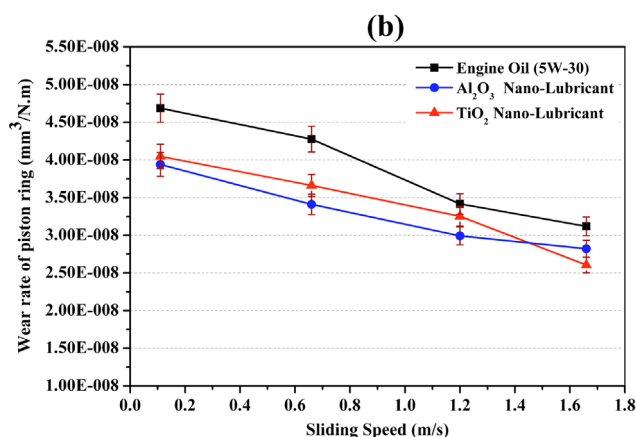
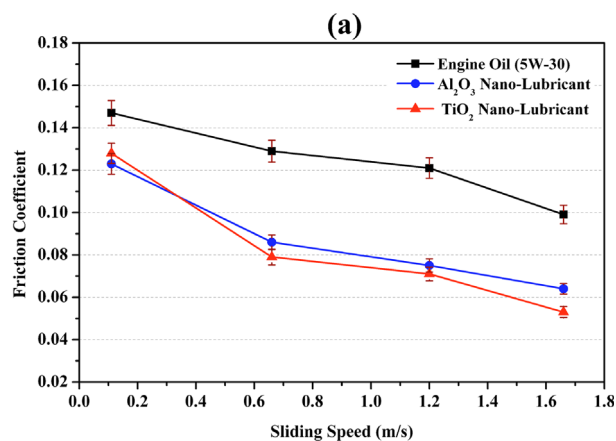


Fig. 11. (a) The variation in the friction coefficient and (b) Wear rate of the ring for various sliding speeds and for a fixed load of 120 N.

sliding speeds for a contact load of 120 N is shown in Fig. 11. The friction coefficient for the use of nano-lubricants was reduced by 35% and 46% for  $\text{Al}_2\text{O}_3$  and  $\text{TiO}_2$  nano-lubricants at an average sliding speed of  $1.66 \text{ m s}^{-1}$ , respectively, (Fig. 11(a)). Furthermore, the wear rate of the ring was reduced by 16% for  $\text{Al}_2\text{O}_3$  and 14% for  $\text{TiO}_2$  nano-lubricants after 25 km sliding in comparison with the lubricant without nanoparticles (Fig. 11(b)). Another significant result as shown in Fig. 11 is the fact that the sliding speed also has an effect on the decrease in friction coefficient and wear rate of the ring for both lubricants with and without nanoparticles.

The main reason for the decrease in friction coefficient and wear rate is the formation of a tribo-film on worn surfaces, acting as a solid lubricant or an ultra-thin lubricating coating, as shown in Fig. 16(a), that decreases shear stress. On the other hand, the rolling action of  $\text{Al}_2\text{O}_3$  and  $\text{TiO}_2$  nanoparticles between the contact surfaces leads to a change from pure sliding friction to rolling friction, a mechanism that provides a decrease in the friction coefficient and the wear. The surface temperature increment with an increase in sliding speed can be attributed to the formation of a stable tribo-film.

### 3.5. Morphologies of worn surfaces and tribo-film formation

In this section, an explanation of the mechanisms supported by experimental evidence has been provided for improve the tribological characteristics of piston ring assembly. Fig. 12 shows the FE-SEM images of the worn surface of the piston ring. The arrows on each image indicate the reciprocating and sliding direction as well as the main features of the topography of the worn surface of the piston ring. It can be observed that the surface morphology of

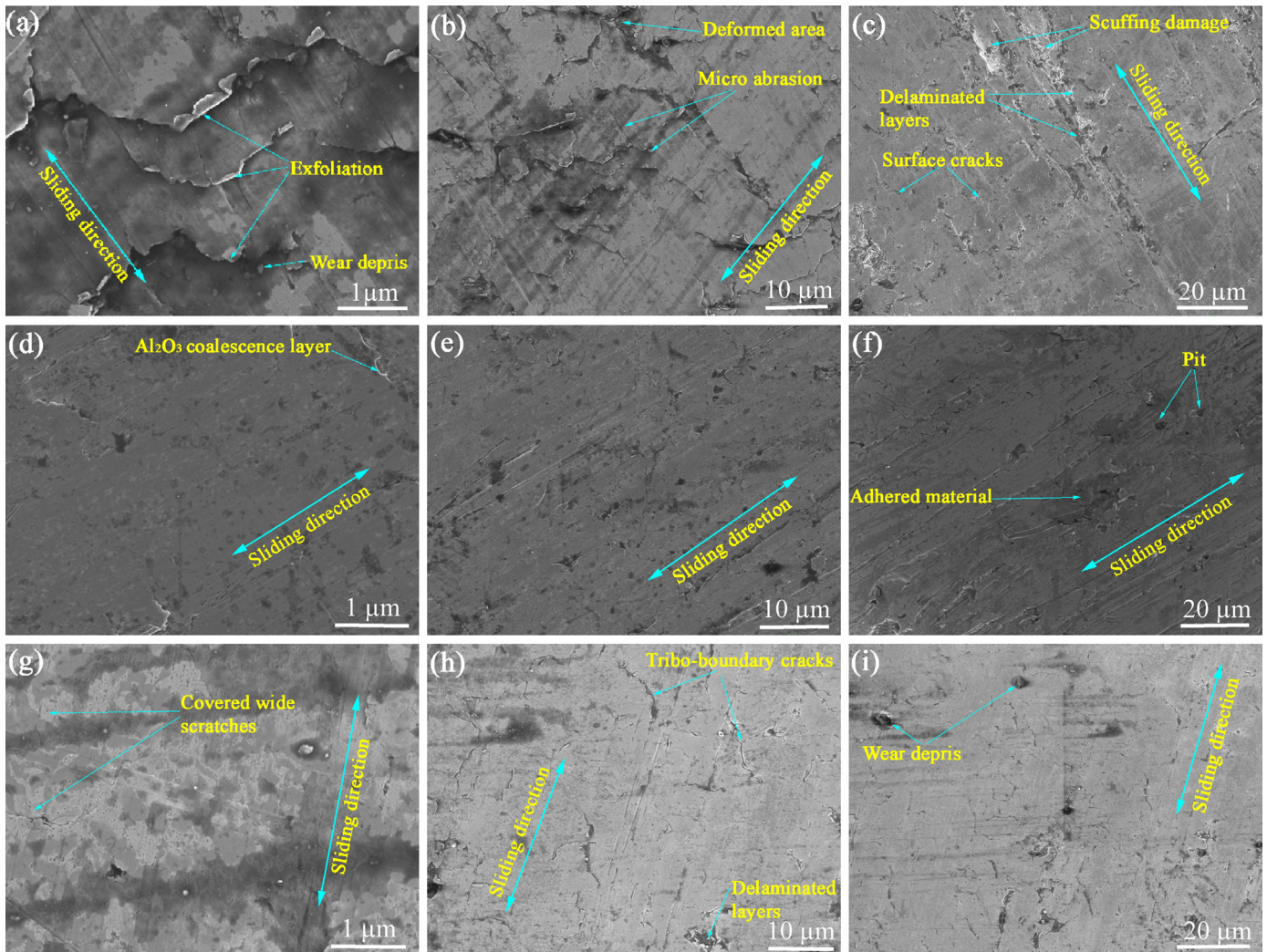


**Fig. 12.** FE-SEM images of the friction surface of the piston ring: (a) Use of engine oil (5W-30); (d) Use of nano-lubricant with 0.25 wt% concentration of  $\text{Al}_2\text{O}_3$ ; (g) Use of nano-lubricant with 0.25 wt% concentration of  $\text{TiO}_2$ ; ((b and c), (e and f), (h and i)) magnified images of a, d, and g, respectively.

the ring for the use of the commercial lubricant (5W-30) without nanoparticle additives showed a large area exfoliation (Fig. 12(a)), micro-plowing on the worn surface (Fig. 12(b)) and scuffing damage (Fig. 12(c)), indicating that severe adhesive wear had occurred. This was due to the penetration of the hard protrusions into the softer surface removing materials by plowing that ultimately led to abrasive wear. Additionally, the increase in the temperature of rubbing surfaces facilitated adhesive wear and plastic deformation causing the dominating flake-like and scuffing damage. The exfoliation, micro-plowing and scuffing damage on the worn surface of the ring confirms the results of high friction coefficient and wear rate, as shown in Fig. 11.

The anti-wear mechanism for  $\text{Al}_2\text{O}_3$  and  $\text{TiO}_2$  nano-lubricants can be explained by considering the situation when the oil film between worn surfaces becomes thinner during the boundary or mixed lubrication regime. Under these conditions, the nanoparticles may carry a portion of the pressure and separate the worn surfaces to prohibit adhesion. However, the formation of a tribo-film on the worn surfaces by nano-lubricants helps in delaying or preventing the beginning of scuffing as shown in Fig. 12 (d and g).

The EDS chemical analysis on worn surfaces of the piston ring and cylinder liner was performed and results are shown in Figs. 13 and 14, respectively. These figures showed the elements analysis of the frictional surfaces lubricated with nano-lubricants containing

$\text{Al}_2\text{O}_3$  and  $\text{TiO}_2$  elements on worn surfaces of the ring and liner. The extent of nanoparticle depositions quantity on the surfaces could be observed in Figs. 13 and 14. An elemental content in EDS analysis showed that the  $\text{TiO}_2$  nanoparticle depositions (1.02–1.25 wt%) lower than  $\text{Al}_2\text{O}_3$  nanoparticle (4.17–5.34 wt%) on worn surfaces, although the  $\text{TiO}_2$  concentration was equal to  $\text{Al}_2\text{O}_3$  concentration (0.25 wt%) in engine oil. This suggested that the  $\text{Al}_2\text{O}_3$  nano-lubricant was more effective in the formation of a tribo-film on worn surface of the ring and hence minimizes the wear rate as shown in Fig. 11(b). In contrast, the  $\text{TiO}_2$  nano-lubricant was more effective in reducing the friction coefficient (Fig. 11(a)) due to a majority of the  $\text{TiO}_2$  nanoparticles remained blended with the engine oil causing mode change of the friction from sliding to rolling friction. This observation may be confirmed by the worn surfaces of the ring and the liner for the use of  $\text{Al}_2\text{O}_3$  nano-lubricant was smoother than the worn surface of the ring and the liner for the use of  $\text{TiO}_2$  nano-lubricant (Fig. 15).

The surface roughness of the frictional surfaces is one of the most significant parameters in controlling the tribological performance in an engine. The surface roughness of the ring and liner were investigated by the 3D optical profilometer before and after tribological tests.  $\text{Al}_2\text{O}_3$  and  $\text{TiO}_2$  nano-lubricants are most effective in reducing the friction coefficient in the boundary lubrication regime at TDC and BDC as shown in Fig. 8. For this reason, the measurement of the surface roughness of the liner was performed

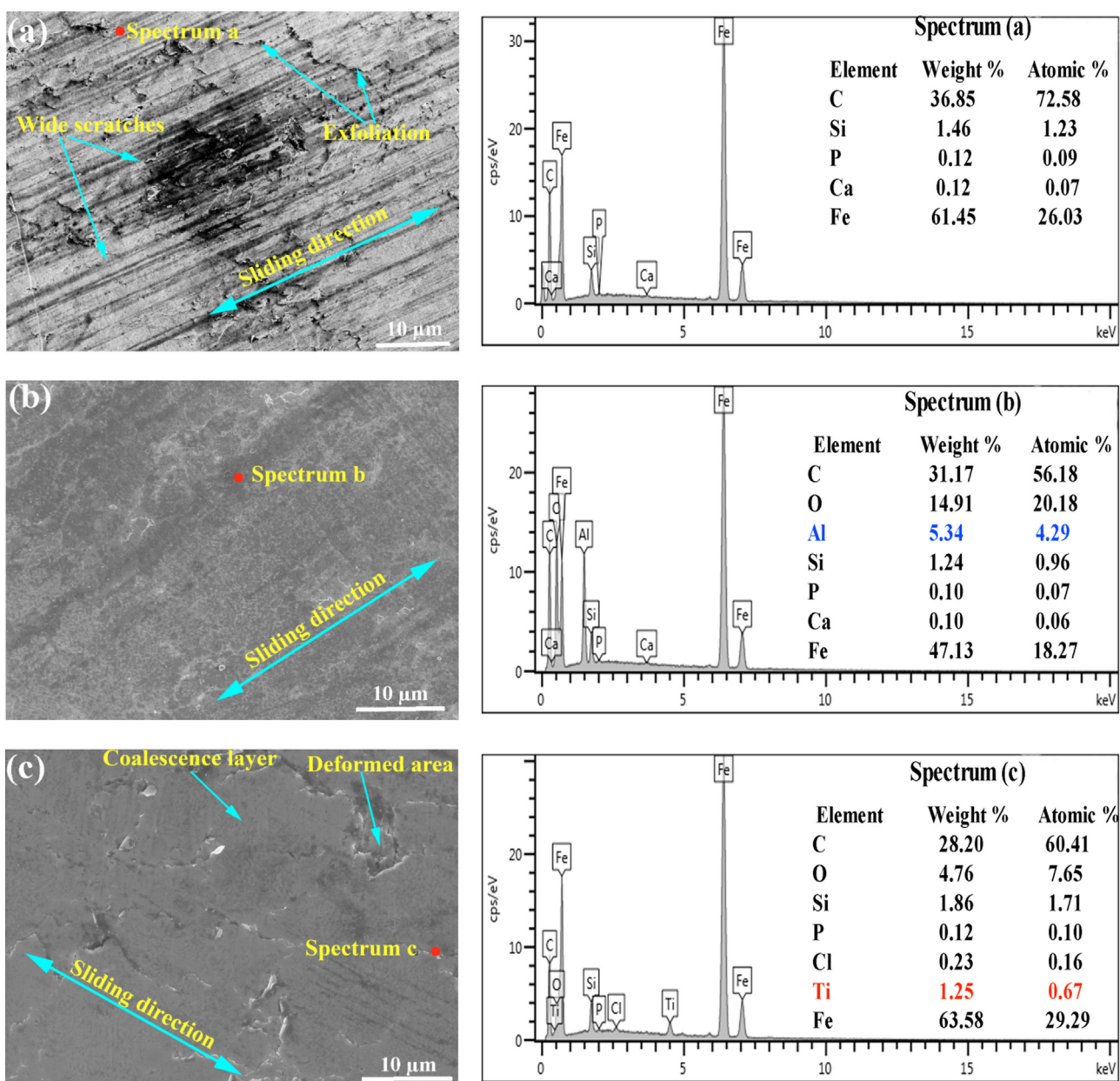


**Fig. 13.** EDS patterns and elemental content of the piston ring surface (a) Use of engine oil (5W-30); (b) Use of nano-lubricant with 0.25 wt% concentration of  $\text{Al}_2\text{O}_3$ , (c) Use of nano-lubricant with 0.25 wt% of  $\text{TiO}_2$ .

at TDC on a large area ( $7.5 \text{ mm} \times 3 \text{ mm}$ ). However, the surface roughness of the ring was measured on a large area ( $5.5 \text{ mm} \times 0.8 \text{ mm}$ ) and not only at one point as shown in Fig. 15. During the tribological tests, the wear had reduced the average surface roughness ( $S_a$ ) of the ring and the liner surfaces because of the abrasion or plastic deformation of the asperities of worn surfaces, as compared to the samples before tests.

The surface roughness values of the worn surfaces and deposition of the nanoparticles on the worn surfaces after tribological tests were diverse and non-uniform at different positions due to a change of the lubrication regimes in these regions. For this reason, we presented the mean values of the surface roughness of the worn surfaces inside of the wear mark measured at different locations as shown in Fig. 16. The results showed that the surface roughness of piston ring was reduced by 49.58% for the case of  $\text{Al}_2\text{O}_3$  and 39.38% for  $\text{TiO}_2$  nano-lubricant. In contrast, the surface roughness of the liner reduced by 14.34% for  $\text{Al}_2\text{O}_3$  and 8.76% for  $\text{TiO}_2$  nano-lubricant, as compared with using engine oil without

nanoparticles. In nano-lubricants, the nanoparticles can fill scars and grooves of the rubbing surfaces (mending and polishing effects) to minimizing surface roughness and asperity contact.

In order to evaluate the tribo-film formation, we studied the worn surface analysis of the ring by FE-SEM, EDS mapping and EDS spectrum for a tribo-film on the cross-section of the worn piston ring surface as shown in Fig. 17 for the use of  $\text{Al}_2\text{O}_3$  nano-lubricant. This figure shows the presence a tribo-film on the worn surface of the ring (Fig. 17(a)). A tribo-film can be formed on the worn surfaces through a chemical reaction and a physical mechanism. In chemical reactions, nano-lubricants that contain active elements such as phosphorus (P), sulfur (S), chlorine (Cl) as shown in Fig. 17(c). These lubricant additives react with surfactant and substrate surface of friction pairs causing the formation of a tribochemical film and deposited in the frictional surfaces of the ring.

Based on the experimental evidence for  $\text{Al}_2\text{O}_3$  nano-lubricant, a trace amount of P and S was detected (active element of ZDDP) as shown Fig. 17(c). This suggests the involvement of  $\text{Al}_2\text{O}_3$

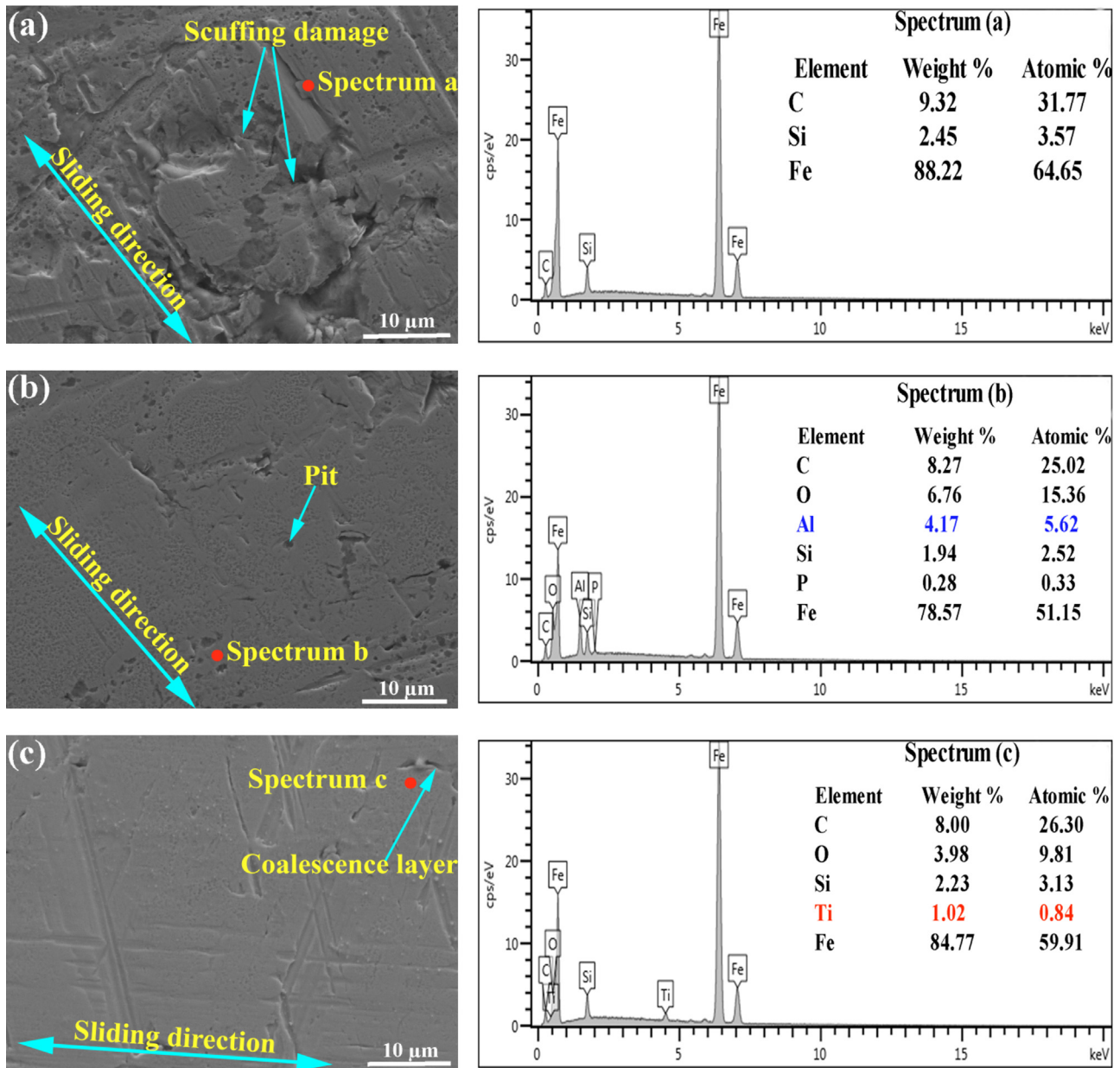


**Fig. 14.** EDS patterns and elemental content of the cylinder liner surface: (a) Use of engine oil (5W-30), (b) Use of nano-lubricant with 0.25 wt% concentration of  $\text{Al}_2\text{O}_3$  (c) Use of nano-lubricant with 0.25 wt% concentration of  $\text{TiO}_2$ .

nanoparticles and oil additive package, specifically zinc dialkyldithio-phosphate (ZDDP) anti-wear additive of the engine oil (5W-30) with the substrate surface to form the tribo-boundary film on the worn surface of the ring. This confirms the synergistic effects between the  $\text{Al}_2\text{O}_3$  nanoparticles and ZDDP. Moreover, the nanoparticles play a dominant role at high temperatures (flash temperature) and pressure during a sliding friction. It is possible that there is thermal activation leading to the lubricity of the nanoparticles, which is most likely related to the chemical interaction with the worn surfaces and the formation of a tribo-film as a solid lubricant. Additionally, a physical film is formed by the mending effect of metal oxide nanoparticles. These nanoparticles in the engine oil can fill scars and grooves of the rubbing surfaces to facilitate the separation, reducing asperity contact.

Furthermore, we analyzed the worn surfaces via XPS to ascertain the composition of tribo-film formed on the worn surface of the piston ring. Fig. 18(a) shows the survey scan and binding energies of  $\text{Al}2\text{p}$ ,  $\text{Si}2\text{p}$ ,  $\text{C}1\text{s}$ ,  $\text{Ca}2\text{p}$ ,  $\text{N}1\text{s}$ ,  $\text{O}1\text{s}$ ,  $\text{Fe}2\text{p}$  and  $\text{Na}1\text{s}$ ,

respectively. The  $\text{O}1\text{s}$  peak at 530.34 eV and the  $\text{C}1\text{s}$  peak at 284.06 eV reveal the existence of carbonyl groups (Fig. 18(d and e)). The  $\text{Fe}2\text{p}$  peak at 709.96 eV indicates that iron is oxidized into  $\text{Fe}_2\text{O}_3$  as shown in Fig. 18(c). The  $\text{Al}2\text{p}$  peak at 73.21 eV demonstrated that  $\text{Al}_2\text{O}_3$  was deposited on the worn surface of the ring (Fig. 18(b)), which is consistent with relevant EDS analysis as shown in Fig. 17. Moreover, the presence of phosphate inside a tribo-film was confirmed by the XPS spectrum, which showed a binding energy of  $\text{P}2\text{p}$  as shown in Fig. 18(f). These results indicate that the tribochemical reaction occurred under these conditions. It is well recognized that the phosphate boundary tribo-film was important for improving the tribological characteristics. From the above analysis on the worn surface of the ring, it is concluded that the boundary tribo-film was mainly composed of  $\text{Al}_2\text{O}_3$  nanoparticles and the oil additive package on the substrate surface.

In summary, the physical mechanism is associated with tribochemical reactions. For achieving effective and successful lubrication mechanism of piston ring assembly in automotive

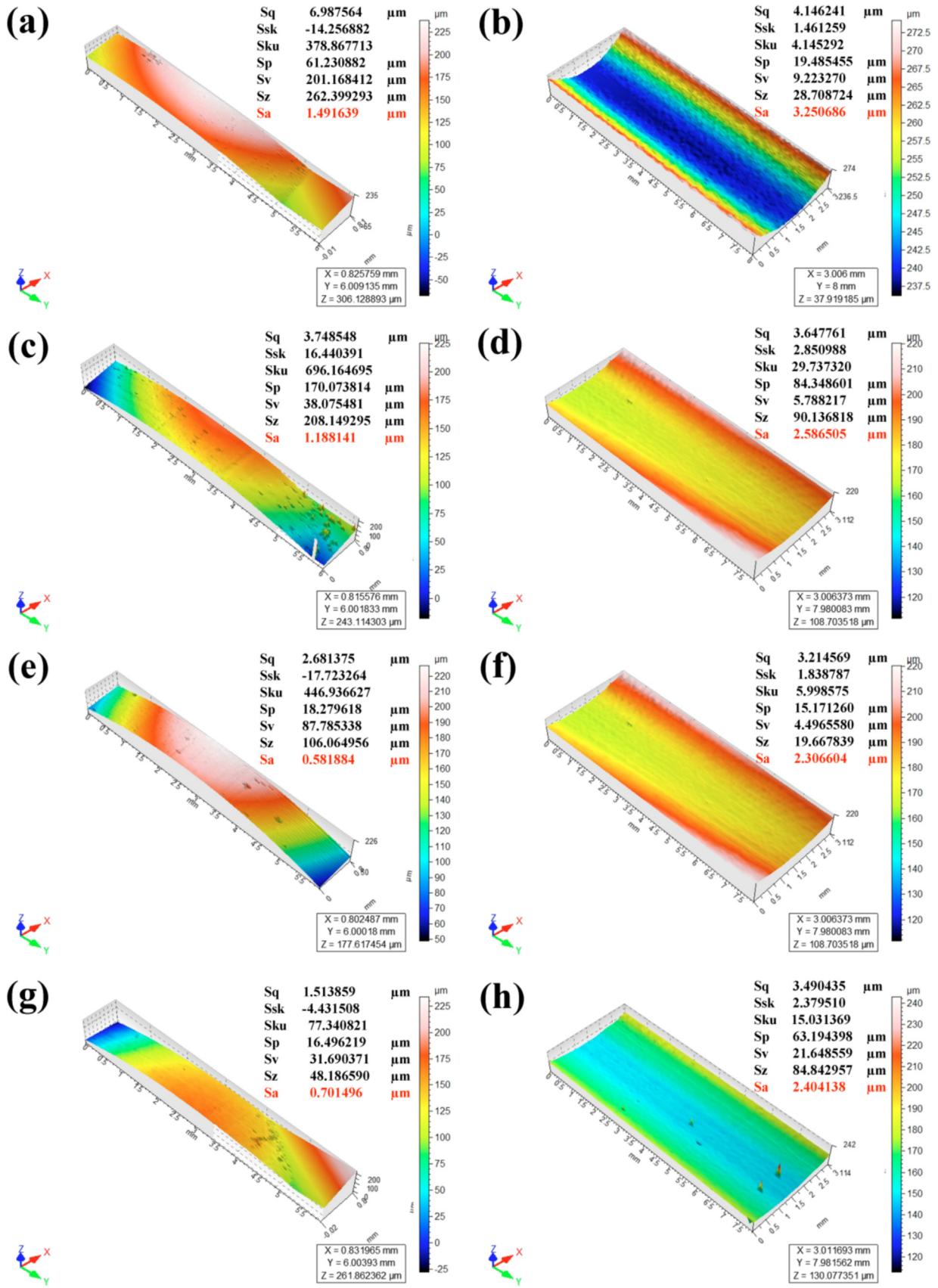


Fig. 15. 3D surface profiler images and height parameters of the piston ring (a, c, e, g) and cylinder liner surface (b, d, f, h); (a, b) Before wear tests, (c, d) Use of engine oil, (e, f) Use of  $\text{Al}_2\text{O}_3$  nano-lubricant, (g, h) Use of  $\text{TiO}_2$  nano-lubricant.

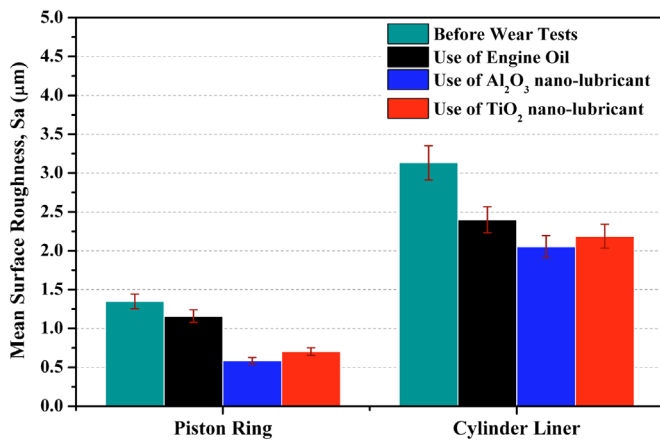


Fig. 16. Comparison of the mean values of the surface roughness at different locations for Al<sub>2</sub>O<sub>3</sub> and TiO<sub>2</sub> nano-lubricants with engine oil (5W-30).

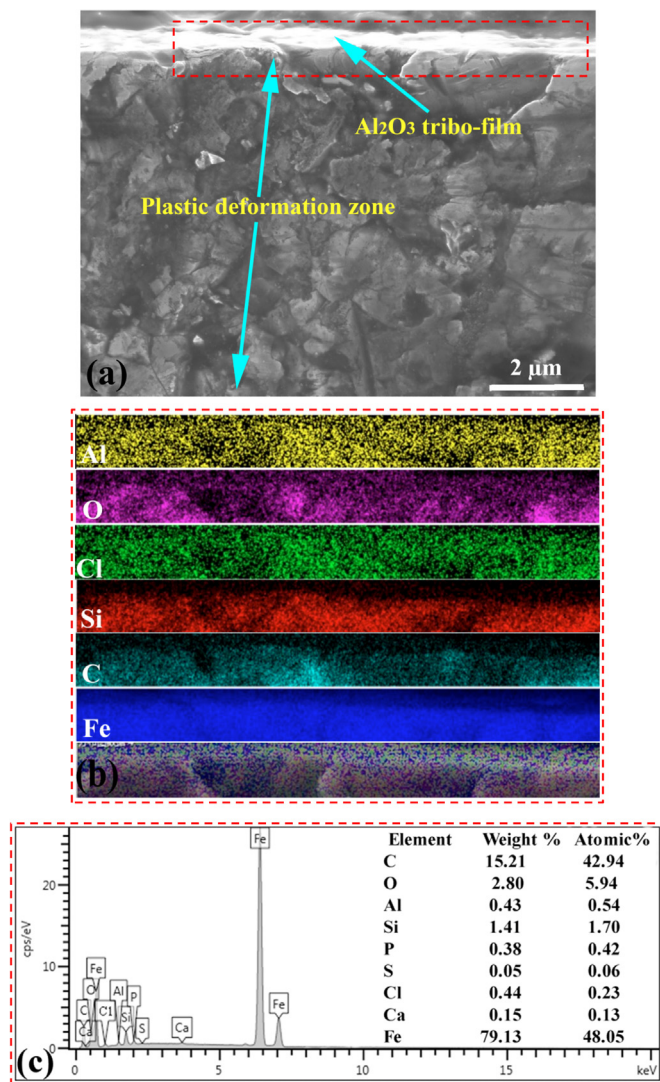


Fig. 17. Formation Al<sub>2</sub>O<sub>3</sub> tribo-boundary film on worn surface of the piston ring surface. (a) FE-SEM imaging on the cross-section, (b) EDS element mapping on tribo-boundary film, (c) EDS spectrum on tribo-boundary film, (b) and (c) corresponding to the red dash line box.

engines, the film formation rate has to be equal to or greater than the film removal rate as well as a strong adhesion and cohesion with substrate surfaces [46]. For this reason, the deposition of a

tribo-film on the worn surfaces is a possible explanation for the improved tribological behavior, which could contribute to a further improvement in the fuel economy in an engine.

#### 4. Conclusions

In the current study, the tribological performance of a piston ring assembly involving the use of Al<sub>2</sub>O<sub>3</sub> and TiO<sub>2</sub> nano-lubricants has been investigated. On the basis of the results presented above, it can be concluded that:

1. The optimum concentration of Al<sub>2</sub>O<sub>3</sub> and TiO<sub>2</sub> nanoparticles blended with the engine oil was 0.25 wt%. Moreover, the addition of oleic acid as a solvent not only aided nanoparticle suspension but also reduced the friction coefficient and wear rate of the ring by 11% and 2.6%, respectively, and could be attributed to the chemical reactions on the frictional surfaces.
2. The kinematic viscosity of Al<sub>2</sub>O<sub>3</sub> and TiO<sub>2</sub> nano-lubricants decreased slightly due to the presence of nanoparticles between the lubricant layers leading to an ease of relative movement with the nanoparticles acting as catalysts. On the other hand, the viscosity index increased with the use of nano-lubricants by 1.86% which could lead to an improved fuel economy in automotive engines.
3. The friction coefficient decreased by 48–50%, 33–44% and 9–13% for the boundary, mixed and hydrodynamic lubrication regimes, respectively, as compared with the use of the engine oil without nanoparticles. This implied that nano-lubricants are most effective in reducing the friction coefficient in the boundary lubrication regime.
4. The frictional power losses were also reduced by 45% and 50% for the Al<sub>2</sub>O<sub>3</sub> and TiO<sub>2</sub> nano-lubricants, respectively. The reduction in friction and power losses could be attributed to the conversion of sliding into rolling friction and the formation of tribo-films on the worn surfaces.
5. The wear rate of the piston ring was reduced by 21–29% for the use of TiO<sub>2</sub> and Al<sub>2</sub>O<sub>3</sub> nano-lubricants respectively, after a 50 km sliding distance, as compared to engine oil without nanoparticles. The anti-wear mechanism was generated by tribo-film through a chemical reaction and a physical mechanism.
6. The surface morphology of the piston ring revealed that nano-lubricant additives resulted in smoother worn surfaces. It is noteworthy that the Al<sub>2</sub>O<sub>3</sub> nano-lubricant was more effective in improving the anti-wear and scuffing resistance via the formation of self-laminating protective films. These protective films could take the form of a solid lubricant or an ultra-thin lubricating coating. Whereas the TiO<sub>2</sub> nano-lubricant was more effective in reducing the friction coefficient. This was because a majority of the TiO<sub>2</sub> nanoparticles remained blended with the engine oil to produce the rolling effect.

#### Notes

The authors declare no competing financial or potential conflict of interest.

#### Acknowledgments

The authors would like to express their deep appreciation to the Hubei Key Laboratory of Advanced Technology for Automotive Components and State Key Laboratory of Advanced Technology for Materials Synthesis and Processing, (Wuhan University of

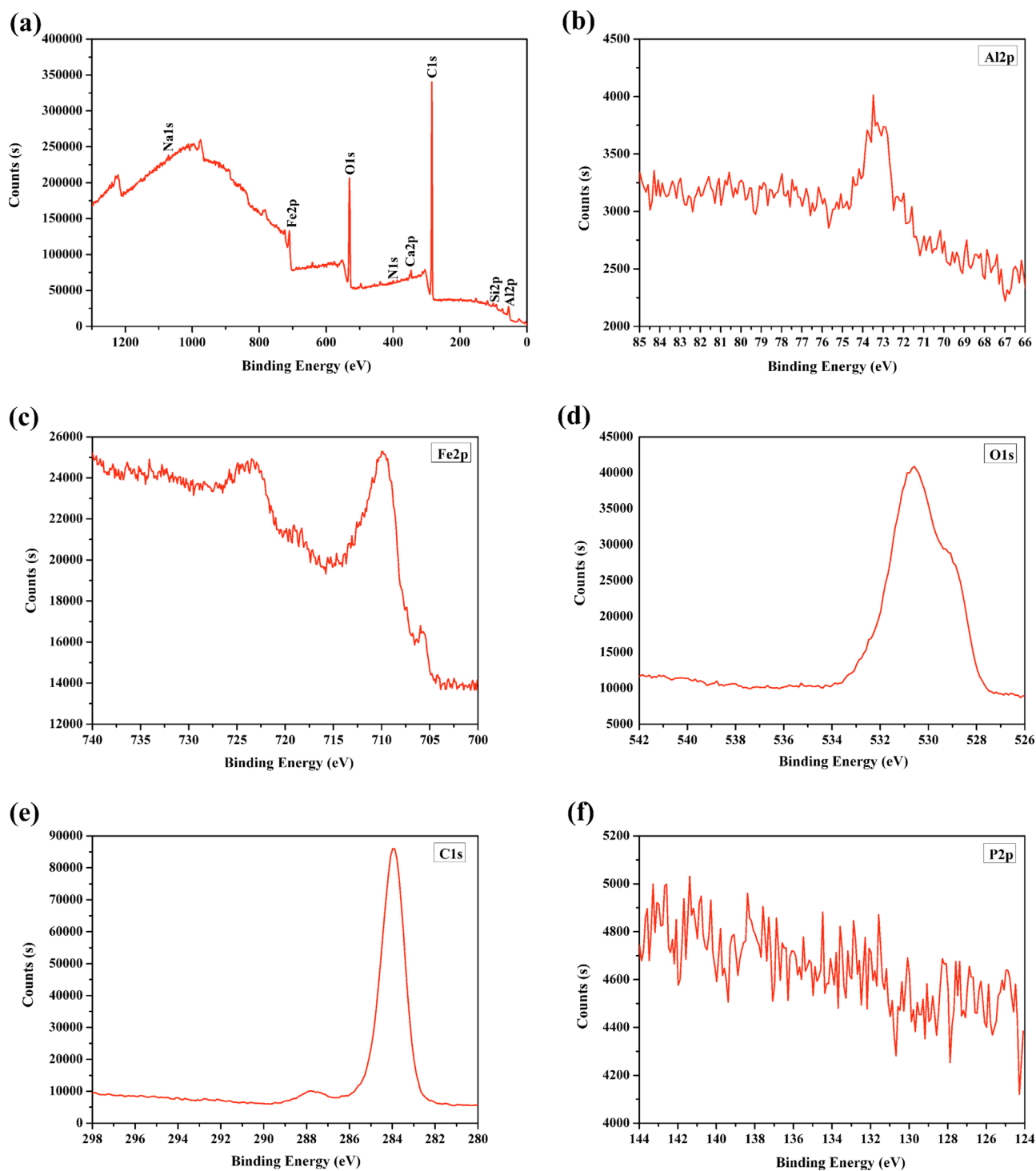


**Fig. 18.** XPS spectra of the boundary tribo-film formed on the worn surface of the piston ring by  $\text{Al}_2\text{O}_3$  nano-lubricant additive; (a) survey scan, (b) Al2p, (c) Fe2p, (d) O1s, (e) C1s and (f) P2p.

Technology) for financial support. M. K. A. Ali and R.F. Turkson acknowledge the Chinese Scholarship Council (CSC) for financial support for their PhD studies in the form of CSC grant Numbers 2014GF032 and 2013GXZ993 respectively. M. K. A. Ali also appreciates the financial support from the Egyptian Government. We also wish to thank the various anonymous reviewers for their helpful and valuable comments.

#### Appendix A. Supporting information

Supplementary data associated with this article can be found in

the online version at <http://dx.doi.org/10.1016/j.triboint.2016.08.011>.

#### References

- [1] Ali MKA, Xianjun H. Improving the Tribological behavior of Internal Combustion Engines via the Addition of Nanoparticles to Engine oils. *Nanotechnol Rev* 2015;4:347–58.
- [2] Ali MKA, Xianjun H, Turkson RF, Ezzat M. An analytical study of tribological parameters between piston ring and cylinder liner in internal combustion engines. *P I Mech Eng, K-J Mul* 2015. <http://dx.doi.org/10.1177/1464419315605922>.

- [3] Lawrence KD, Ramamoorthy B. Multi-surface topography targeted plateau honing for the processing of cylinder liner surfaces of automotive engines. *Appl Surf Sci* 2016;365:19–30.
- [4] Choi Y, Lee C, Hwang Y, Park M, Lee J, Choi C, Jung M. Tribological behavior of copper nanoparticles as additives in oil. *Curr Appl Phys* 2009;9:124–7.
- [5] Chang H, Li Z, Kao M, Huang K, Wu H. Tribological property of TiO<sub>2</sub> nanolubricant on piston and cylinder surfaces. *J Alloy Compd* 2010;495:481–4.
- [6] Senatore A, Aleksandric D. Advances in piston rings modelling and design. *Recent Patents Eng* 2013;7:51–67.
- [7] Mai L, Dong Y, Xu L, Han C. Single nanowire electrochemical devices. *Nano Lett* 2010;10:4273–8.
- [8] Dai W, Kheireddin B, Gao H, Liang H. Roles of nanoparticles in oil lubrication. *Tribol Int* 2016;102:88–98.
- [9] Ali MKA, Xianjun H, Turkson R, Peng Z, Chen X. Enhancing the thermophysical properties and tribological behaviour of engine oils using nano-lubricant additives. *RSC Adv* 2016. <http://dx.doi.org/10.1039/C6RA10543B>.
- [10] Boshui C, Ke Cheng G, Jianhua F, Jiang W, Jiu W, Nan Z. Tribological characteristics of monodispersed cerium borate nanospheres in biodegradable rapeseed oil lubricant. *Appl Surf Sci* 2015;353:326–32.
- [11] Hsu SM, Gates R. Boundary lubricating films: formation and lubrication mechanism. *Tribol Int* 2005;38:305–12.
- [12] Zhang Y, Tang H, Ji X, Li C, Chen L, Zhang D, Yang X, Zhang H. Synthesis of reduced graphene Oxide/CU Nanoparticle Composites and Their Tribological properties. *RSC Adv* 2013;3:26086–93.
- [13] Lin LY, Kim DE, Kim WK, Jun SC. Friction and wear characteristics of multi-layer graphene films investigated by atomic force microscopy. *Surf Coat Tech* 2011;205:4864–9.
- [14] Bahramian A, Raeissi K, Hakimzad A. An investigation of the characteristics of Al<sub>2</sub>O<sub>3</sub>/TiO<sub>2</sub> PEO nanocomposite coating. *Appl Surf Sci* 2015;351:13–26.
- [15] Ingole S, Charanpahari A, Kakade A, Umare SS, Bhatt DV, Menghani J. Tribological behavior of nano TiO<sub>2</sub> as an additive in base oil. *Wear* 2013;301:776–85.
- [16] Shenoy B, Binu K, Pai R, Rao D, Pai RS. Effect of nanoparticles additives on the performance of an externally adjustable fluid film bearing. *Tribol Int* 2012;45:38–42.
- [17] Kao MJ, Lin CR. Evaluating the role of spherical titanium oxide nanoparticles in reducing friction between two pieces of cast iron. *J Alloys Compd* 2009;483:456–9.
- [18] Arumugam S, Sriram G. Preliminary study of nano and microscale TiO<sub>2</sub> additives on tribological behavior of chemically modified rapeseed oil. *Tribol Trans* 2013;56:797–805.
- [19] N Mohan, M Sharma, R Singh, N Kumar. Tribological properties of automotive lubricant SAE 20W40 containing nano-Al<sub>2</sub>O<sub>3</sub> particles. *SAE Technical Paper* 2014-01-2781 2014;doi:10.4271/2014-01-2781.
- [20] McElwain SE, Blanchet TA, Schadler LS, Sawyer WG. Effect of particle size on the wear resistance of alumina-filled PTFE micro and nano composites. *Tribol Trans* 2008;51:247–53.
- [21] Yadgarov L, Petrone V, Rosentsveig R, Feldman Y, Tenne R, Senatore A. Tribological studies of rhenium doped fullerene-like MoS<sub>2</sub> nanoparticles in boundary, mixed and elasto-hydrodynamic lubrication conditions. *Wear* 2013;297:1103–10.
- [22] Rapoport L, Moshkovich A, Perflyev V, Laikhtman A, Lapsker I, Yadgarov L, Tenne R. High lubricity of re-doped fullerene-like MoS<sub>2</sub> nanoparticles. *Tribol Lett* 2012;45:257–64.
- [23] Gulzar M, Masjuki H, Varman M, Kalam M, Mufti R, Zulkifli N, Yunus R, Zahid R. Improving the AW/EP ability of chemically modified palm oil by adding CuO and MoS<sub>2</sub> nanoparticles. *Tribol Int* 2015;88:271–9.
- [24] Luo T, Wei X, Huang X, Huang L, Yang F. Tribological properties of Al<sub>2</sub>O<sub>3</sub> nanoparticles as lubricating oil additives. *Ceram Int* 2014;40:7143–9.
- [25] Wu Y, Tsui W, Liu T. Experimental analysis of tribological properties of lubricating oils with nanoparticle additives. *Wear* 2007;262:819–25.
- [26] Vasheghani M, Marzbanrad E, Zamani C, Aminy M, Raissi B, Ebadzadeh T, Barzegar-Bafroei H. Effect of Al<sub>2</sub>O<sub>3</sub> phases on the enhancement of thermal conductivity and viscosity of nanofluids in engine oil. *Heat Mass Transfer* 2011;47:1401–5.
- [27] Tang Z, Li S. A review of recent developments of friction modifiers for liquid lubricants (2007–present). *Curr Opin Solid S M* 2014;18:119–39 [31].
- [28] Tadmor R, Rosensweig RE, Frey J, Klein J. Resolving the puzzle of ferrofluid dispersants. *Langmuir* 2000;16:9117–20.
- [29] ASTM G181-11. Standard test method for conducting friction tests of piston ring and cylinder liner materials under lubricated conditions. *ASTM Int*; 2004.
- [30] ASTM E92-82. Standard test method for vickers hardness of metallic materials. *ASTM Int*; 2003.
- [31] Obert P, Müller T, Füller HJ, Bartel D. The influence of oil supply and cylinder liner temperature on friction, wear and scuffing behavior of piston ring cylinder liner contacts—A new model test. *Tribol Int* 2016;94:306–14.
- [32] Morina A, Lee P, Priest M, Neville A. Challenges of simulating fired engine ring-liner oil additive/surface interactions in ring-liner bench tribometer. *Tribol-Mater. Surfaces Interfaces* 2011;5:25–33.
- [33] Akalin O, Newaz GM. Piston ring-cylinder bore friction modeling in mixed lubrication regime: Part II—Correlation with bench test data. *J Tribol* 2001;23:219–23.
- [34] Truhan JJ, Qu J, Blau PJ. A rig test to measure friction and wear of heavy duty diesel engine piston rings and cylinder liners using realistic lubricants. *Tribol. Int.* 2005;38:211–8.
- [35] D'Agostino V, Senatore A. Fundamentals of lubrication and friction of piston ring contact. In: Rahnejat H, editor. *Tribology and Dynamics of Engine and Powertrain: Fundamentals, Applications and Future Trends*. Cambridge, UK: Woodhead Publishing Ltd; 2010. p. 357–71.
- [36] Priest M, Dowson D, Taylor CM. Predictive wear modelling of lubricated piston rings in a diesel engine. *Wear* 1999;231:89–101.
- [37] Baker CE, Theodossiades S, Rahnejat H, Fitzsimons B. Influence of in-plane dynamics of thin compression rings on friction in internal combustion engines. *J Engin. Gas Turbines Power* 2012;134:092801.
- [38] Thamaphat K, Limsuwan P, Ngotawornchai B. Phase Characterization of TiO<sub>2</sub> Powder by XRD and TEM. *Kasetsart J (Nat Sci)* 2008;42:357–61.
- [39] Loehle S, Matta C, Minfray C, Mogné TL, Martin JM, et al. Mixed lubrication with C18 fatty acids: effect of unsaturation. *Tribol. Lett.* 2014;53:319–28.
- [40] Wei L, Jian-Hua Z, Jian-Hua Q. Application of nano-nickel catalyst in the viscosity reduction of Liaohe extra-heavy oil by aqua-thermolysis. *J Fuel Chem Technol* 2007;35:176–80.
- [41] Timofeeva EV, Routbort JL, Singh D. Particle shape effects on thermophysical properties of alumina nanofluids. *J Appl Phys* 2009;106:014304.
- [42] Zhao B, Dai XD, Zhang ZN, Xie YB. A new numerical method for piston dynamics and lubrication analysis. *Tribol Int* 2016;94:395–408.
- [43] Craciun AD, Gallani JL, Rastei MV. Stochastic stick-slip nanoscale friction on oxide surfaces. *Nanotechnology* 2016;27:055402.
- [44] Brandão JA, Meheux M, Ville F, Seabra JH, Castro J. Comparative overview of five gear oils in mixed and boundary film lubrication. *Tribol Int* 2012;47:50–61.
- [45] Zin V, Agresti F, Barison S, Colla L, Gondolini A, Fabrizio M. The synthesis and effect of copper nanoparticles on the tribological properties of lubricant oils. *Nanotechnology* 2013;12:751–9.
- [46] Ratoí M, Niste VB, Alghawel H, Suen YF, Nelson K. The impact of organic friction modifiers on engine oil tribofilms. *RSC Adv* 2014;4:4278–85.